Cancer Letters 446 (2019) 103–111

Contents lists available at ScienceDirect

Cancer Letters

journal homepage: www.elsevier.com/locate/canlet

Original Articles

$Kras^{G12D}$ mutation contributes to regulatory T cell conversion through activation of the MEK/ERK pathway in pancreatic cancer

He Cheng[a,b,c,1], Kun Fan[a,b,c,1], Guopei Luo[a,b,c,1], Zhiyao Fan[a,b,c], Chao Yang[a,b,c], Qiuyi Huang[a,b,c], Kaizhou Jin[a,b,c], Jin Xu[a,b,c], Xianjun Yu[a,b,c,**], Chen Liu[a,b,c,*]

[a] Department of Pancreatic Surgery, Fudan University Shanghai Cancer Center, Shanghai, China
[b] Department of Oncology, Shanghai Medical College, Fudan University, Shanghai, China
[c] Shanghai Pancreatic Cancer Institute, Shanghai, China

ARTICLE INFO

Keywords:
Pancreatic cancer
Immunosuppressive
$Kras^{G12D}$ mutation
IL-10
TGF-β

ABSTRACT

Genetic alterations have been attributed to the abnormal immune microenvironment in cancer. However, the relationship between the $Kras^{G12D}$ mutation and regulatory T cells (Tregs) in pancreatic cancer remains unclear. In this study, we found that $Kras^{G12D}$ mutation status as determined by ddPCR correlated with high levels of Treg infiltration in resectable pancreatic cancer tissues. Compared to wild-type tumour cells, tumours cells with the $Kras^{G12D}$ mutation were associated with higher levels of Tregs, and knockout of the $Kras^{G12D}$ mutation reversed this effect. In addition, overexpression of the $Kras^{G12D}$ mutation in wild-type Kras tumour cells resulted in conversion of $CD4^+CD25^-$ T cells into Tregs. We also found that in tumour cells, the $Kras^{G12D}$ mutation activated the MEK/ERK pathway, thereby up-regulating the levels of interleukin-10 (IL-10) and transforming growth factor-β (TGF-β), which induced Treg conversion. In summary, $Kras^{G12D}$ mutation plays a critical role in Treg conversion and contributes to an immunosuppressive tumour microenvironment in pancreatic cancer. These results provide new insights into the relationship between gene mutation and immune escape.

1. Introduction

Pancreatic cancer remains the fourth leading cause of cancer-related death worldwide and has an extremely poor prognosis [1]. Pancreatic cancer is often accompanied by oncogenic driver mutations in genes such as Kras, TP53, Smad4, and CDKN2A. Of these four driver genes, Kras is the most frequently mutated gene, and mutated Kras is found in 70%–95% of pancreatic cancer cases [2]. Mutations in Kras play a vital role in pancreatic cancer initiation and progression, but, targeted therapy against Kras or related downstream signalling pathways has nearly always failed to show survival benefits [3].

Immune disorder is one of the most important hallmarks of cancer. Pancreatic cancer is characterised by a dense stroma and abnormal immune cell infiltration, which is associated with immunosuppressive conditions that facilitate the escape of tumour cells from immune cells [4,5]. Regulatory T cells (Tregs) are typical immunosuppressive T cells that play a key role in immune homeostasis. Tregs increase the secretion of various immunosuppressive cytokines, inhibiting cytotoxic lymphocyte function and contributing to immune escape [6]. Tumour-infiltrating Tregs, as well as the proportion of peripheral Tregs, are independent prognostic factors in many cancers, including pancreatic cancer [7–9].

Tumour cells present tumour-associated antigens on their cell surface that are derived from mutated Kras, however, the immune system fails to kill tumour cells with mutated Kras [10]. This phenomenon can be explained by the abnormal immunosuppressive tumour microenvironment. Mutated Kras is reportedly associated with Treg induction in colon cancer and lung cancer [11]. However, the exact role of Kras mutation in Treg conversion in pancreatic cancer is still not well understood. Accordingly, this study investigated the correlation between the $Kras^{G12D}$ mutation and Tregs in pancreatic cancer tissues as well as the potential mechanisms underlying this correlation.

2. Materials and methods

2.1. Cell culture

Human pancreatic cancer cells, Bxpc-3 and SW1990, and 293T cells

* Corresponding author. Department of Pancreatic Surgery, Shanghai Cancer Center, Fudan University, 270 DongAn Road, Xuhui, Shanghai 200032, PR China.
** Corresponding author. Department of Pancreatic Surgery, Shanghai Cancer Center, Fudan University, 270 DongAn Road, Xuhui, Shanghai 200032, PR China.
E-mail addresses: yuxianjun@fudanpci.org (X. Yu), liuchen@fudanpci.org (C. Liu).
[1] These authors contributed equally to this article.

https://doi.org/10.1016/j.canlet.2019.01.013
Received 14 October 2018; Received in revised form 4 December 2018; Accepted 10 January 2019

were purchased from the American Type Culture Collection (ATCC). All cells were cultured with DMEM or 1640 medium with 10% foetal bovine serum in a 37 ˚C incubator and 5% CO_2 culture conditions.

2.2. Pancreatic cancer tissue samples

Pancreatic cancer tissue samples used in this study were obtained from Fudan University Shanghai Cancer Center from 2012 to 2013. The basic clinico-pathological parameters of these patients was described in Supplementary table 1. Diagnosis of all pancreatic cancer samples was histologically confirmed by experienced pathologists. This study was approved by the Clinical Research Ethic Committee of Shanghai Cancer Center of Fudan University, and informed consent was obtained from all patients.

2.3. Detection of the $Kras^{G12D}$ mutation using droplet digital PCR (ddPCR)

We enriched 64 formalin-fixed paraffin-embedded (FFPE) tissue samples for tumour tissue by macrodissection with scalpels, guided by a contiguous haematoxylin and eosin (H&E) section. The QIAamp DNA FFPE Tissue Kit (Qiagen) was used to extract genomic DNA following the manufacturer's instructions. DNA quality and quantity were assessed by the Qubit® 2.0 Fluorometer (Life Technologies) and gel electrophoresis. $Kras^{G12D}$ mutation status was assessed using a ddPCR system (Bio-Rad Laboratories, Hercules, CA). Briefly, the primers (Kras-G12D-Forward primer: TGCTGAAAATGACTGAATATAAACTTGTG and Kras-G12D-Rrverse primer: AGCTGTATCGTCAAGGCACTCTT) and probe (Kras-G12D-Probe: TGGAGCTGATGGCGT) for detecting the $Kras^{G12D}$ mutation were obtained following a standard protocol (Bio-Rad Laboratories). The PCR mixture was added into the droplet generation cartridge, and approximately 20,000 monodispersed droplets were prepared for each sample using the QuantaLife droplet generator. The water-in-oil emulsions were then transferred to a 96-well PCR plate for the next step of amplification cycles. The experimental steps were described in detail previously [12]. For ddPCR determination of thresholds, the result was considered positive when PCR monodispersed droplets had a fluorescence signal and negative when they had no fluorescence signal. The concentrations (copy numbers) of targets in the samples were measured by QuantaSoft software.

2.4. Antibodies and reagents

p-ERK1/2 antibody (Cat. #4370), ERK1/2 antibody (Cat. #4695), and ERK antibody (Cat. #4695) were purchased from Cell Signalling Technology (Beverly, MA, USA). Kras antibody (Cat. #ab180772), IL-10 ELISA kit (Cat. #ab100549), and TGF-β ELISA kit (Cat. #ab100647) were purchased from abcam (Cambridge, MA, USA). IL-10 cytokine (Cat. #CD04, Novoprotein), TGF-β cytokine (Cat. #CA59, Novoprotein), and IL-2 cytokine (Cat. #C013) were purchased from Novoprotein (USA). MojoSort™ Human $CD4^+$ T cell isolation Kit (Cat. #480010), MojoSort™ Buffer (Cat. #480017), CD3 antibody (Cat. #300313), CD28 antibody (Cat. #302913), FITC-CD4 antibody (Cat. #300505), APC-CD25 antibody (Cat. #302609), PE-Foxp3 (Cat. #320007), and True-Nuclear Transcription Factor Buffer Set (Cat. #424401) were purchased from Biolegend (San Diego, CA, USA). PD98059 (Cat. #HY-12028, MCE) was purchased from MedChemExpress. The siRNAs of TGF-β and IL-10 were synthesized (Genepharma Corp, Shanghai, China) and the sequences are as follows. The TGF-β siRNA sense: CAAGCAGAGUACACACAGCAU, anti-sense: AUGCUGUGUGUACUCUGCUUG. The IL-10 siRNA sense: GCAGGUGA AGAAUGCCUUUAA, anti-sense: UUAAAGGCAUUCUUCACCUGC.

2.5. Western blotting

Pancreatic cancer cells were collected for protein extraction. Briefly, cells were washed with pre-cooled PBS, then lysed with RIPA lysis buffer (50 mM Tris-HCl, pH 7.4, 150 mM NaCl, 1% NP-40, 0.1% SDS, 1 mM EDTA) with protease inhibitor (1 mM Na3VO4, 1 mM PMSF) on ice for 30 min. The cell lysate was centrifuged at 12,000 rpm for 10 min at 4 ˚C. The protein concentration was determined by a BCA assay kit (KANGWEI, Shanghai, China, Cat. #CW0014S). The protein loading samples were prepared with the same protein mass and sample volume. Then, the protein samples were separated by SDS-PAGE, transferred onto nitrocellulose membranes, and blocked with 5% non-fat milk in PBST for 1 h at room temperature. Primary antibodies were incubated overnight at 4 ˚C. After washing with PBST three time for 10 min each, secondary antibodies were incubated for 1 h at room temperature and then washed with PBST three time for 10 min every time. Detected proteins were visualized using an enhanced chemiluminescence system.

2.6. Enzyme-linked immunosorbent assay (ELISA)

ELISAs for IL-10 and TGF-β were performed according to the manufacturer's instructions. Briefly, standard samples and cell supernatants were added into wells with IL-10 or TGF-β antibody coating. Then, plates were covered and incubated for 2 h at room temperature. Then, the liquid was poured out, and the plates were washed with washing buffer five times. IL-10 or TGF-β conjugate was added to the wells and incubated for 2 h at room temperature. Then, liquid was poured out, and plates were washed five time to completely remove liquid. Substrate solution was added and incubated for 20 min at room temperature in the dark. Then, 50 μl stop solution was added to terminate the reaction. Finally, results were detected by a microplate reader at 450 nm.

2.7. Real-time PCR

Total RNA was isolated using Trizol (Invitrogen, NY, USA, Cat. #15596026), and reverse transcription was performed using the Promega reverse transcription kit according to the manufacturer's instructions. Total RNA concentration was assayed and reverse transcribed into cDNA. Real-time PCR was performed using SYBR Green (Takara, Japan) to analyse IL-10 and TGF-β mRNA levels. The reaction mixture included 4.5 μl cDNA (100 ng/μl), 5 μl 2xSYBR mix, 0.2 μl forward and reverse primers, and 0.1 μl ROX to a total volume of 10 μl. Real-time PCR results were calculated after at least three time independent experiments. The forward primer for IL-10 was GGCGCTG TCATCGATTTCTTC, and the reverse primer was TAGAGTCGCCACCC TGATGT. TGF-β forward primer was ACAGCAACAATTCCTGGCGA, and the reverse primer was GTAGTGAACCCGTTGATGTCCA. GAPDH forward primer was TCGGAGTCAACGGATTTGT, and reverse primer was TTCCCGTTCTCAGCCTTGAC.

2.8. Establishment of Kras knockout and $Kras^{G12D}$ cells

To establish cells with stable $Kras^{G12D}$ knockout, the lentiCRISPR was employed. The target sequence1 and sequence2 of Kras was sgKras1: CGCTCGCTCCCAGTCCGAAA and sgKras2: TCGCTCCCAGTC CGAAATGG, respectively. The sgKras1 and sgKras2 sequences were cloned into the lentiCRISPR vector according to the protocol. The Kras knockout plasmid (with lentiCRISPR as control) or $Kras^{G12D}$ overexpression plasmid (with pCDH vector as control) was co-transfected into 293T cells with the packaging plasmids pVSVg and psPAX2 to make lentivirus. Cell supernatant was collected and filtered with 0.45 μm filters. Lentivirus was added into cultured pancreatic cancer cells, and cells were screened by puromycin selection. To establish stable cell lines, cells were divided into 96-well plates with one cell in each well. Knockout efficiency was determined by Western blotting.

2.9. Immunohistochemical staining

Immunohistochemistry (IHC) was performed as previously

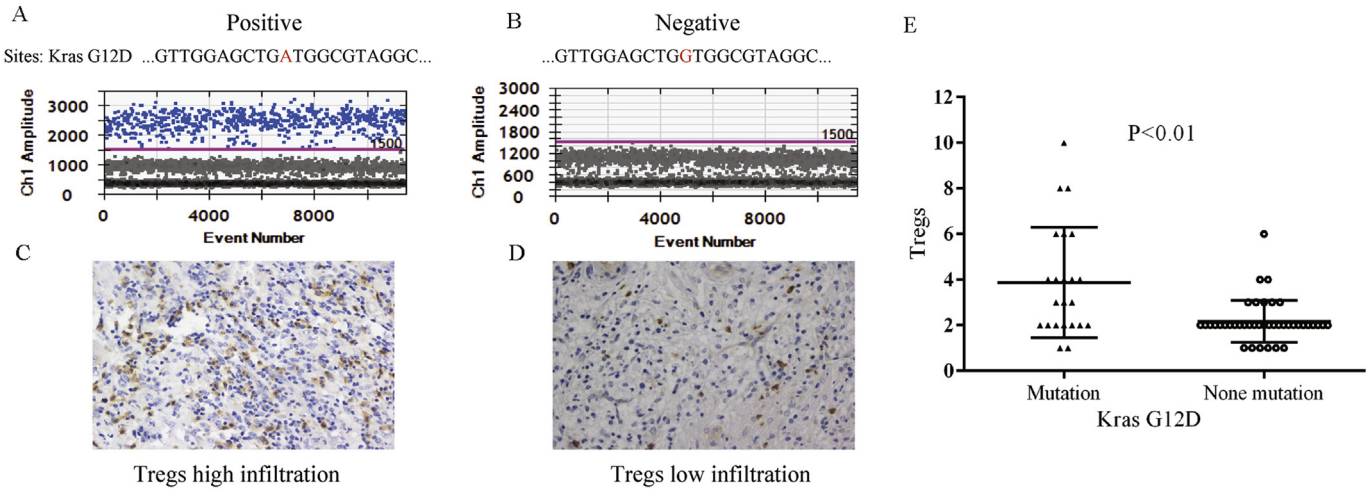

Fig. 1. Kras^{G12D} mutation is associated with enhanced Treg infiltration in pancreatic cancer tissues. (A) and (B) Example of Kras^{G12D} mutation or no mutation in pancreatic cancer tissues detected by ddPCR. (C) and (D) Example of high Treg infiltration or low infiltration in pancreatic cancer tissues. (E) Kras^{G12D} mutation was correlated with high Treg infiltration in 64 pancreatic cancer tissues.

described [13]. IHC results were scored according to the percentage and intensity of positive cells. The percentage of positive cells was divided into five grades: < 10% (0), 10–25% (1), 25–50% (2), 50–75% (3), and > 75% (4). Staining intensity was divided into four grades: no staining (0), light brown (1), brown (2), and dark brown (3). IHC results were divided into –, +, ++ and +++, indicating negative, weakly positive, positive and strongly positive, respectively.

2.10. CD4$^+$ T cell isolation using MojoSort™ isolation kit

CD4$^+$ T cells were isolated by using a MojoSort™ Isolation Kit's Protocol (Biolegend). Briefly, peripheral blood mononuclear cells (PBMCs) were isolated from blood samples. Then, PBMCs were re-suspended in MojoSort™ Buffer, counted, and adjusted at 1*10^8 cells/ml. Next, 100 µl cell suspension (10^7 cells) was added into a new tube, and 10 µl biotin-antibody cocktail was added. The mixture was incubated on ice for 15 min, and 10 µl beads was added by vortex and incubated on ice for 15 min. Sorting buffer was added, and the sample was placed in the magnet for 5 min, followed by collection of liquid. Unlabelled fractions were CD4$^+$ T cell subgroups to which sorting buffer was added once more to isolate additional CD4$^+$ T cells.

2.11. Co-culture of CD4 + T cells and pancreatic cancer cells

First, 24-well plates were coated with CD3 antibody at 4 µg/ml in 0.5 ml total volume for per well overnight at 4 °C. Isolated CD4 + T cells were counted and approximately 1 × 10^6 cells per well were added to culture. Next, 1 µg/ml CD28 and 100–200 U/ml IL-2 were simultaneously added for culture. After 48 h, CD4 + T cells were plated into wells in which pancreatic cancer cells had been seeded the day before. CD4$^+$ T cells were co-cultured with cancer cells for 4–5 days. At that time, CD4$^+$ T cells were collected and washed with PBS, then strained for flow cytometry analysis.

2.12. Analysis of tumour-associated Tregs using flow cytometry

Analysis of tumour-associated Tregs by flow cytometry was performed according to the True-Nuclear™ Transcription Factor Staining Protocol (Biolegend). Briefly, cultured T cells were collected, washed, and incubated with 5 µl of FITC-CD4 antibody and 5 µl of APC-CD25 antibody on ice for 20 min in the dark. Then, 1 ml of Transcription Factor 1*Fix solution was added, and the mixture was incubated at room temperature for 60 min in the dark. Next, 2 ml Transcription Factor 1*Perm Buffer was added and centrifuged at 400 × *g* at 4 °C for 5 min, followed by removal of the supernatant. Cells were resuspended in 100 µl Transcription Factor Perm Buffer, and PE-Foxp3 antibody was incubated for 30 min on ice, avoiding light. Then, 2 ml Perm Buffer was added, the sample was centrifuged at 400 × *g* at 4 °C for 5 min, and the supernatant was removed. The cells were washed with PBS and centrifuged at 400 × *g* at 4 °C for 5 min. The supernatant was removed, and cells were detected by flow cytometry. The first step was to gate living naïve T cells via forward scatter (FSC) and side scatter (SSC). The second step was to gate CD4 positive T cells. The third step was to gate both CD25 and Foxp3 positive cells from the CD4 positive cell subpopulation as Tregs and analyse the proportion of Tregs. Statistical analyses were performed on a minimum of 10,000 events gated on the population of interest.

3. Results

3.1. Kras^{G12D} mutation correlates with Treg infiltration in resectable pancreatic cancer tissues

To investigate the potential correlation between the Kras^{G12D} mutation and Treg infiltration in pancreatic cancer tissues, we assessed Kras^{G12D} mutation in 64 resectable pancreatic cancer specimens by ddPCR (Fig. 1A and B) and found that 23 of the 64 (36%) specimens were positive for the mutation. We also measured Foxp3-positive lymphocytes in matched tissue samples using immunohistochemistry (Fig. 1C and D). Interestingly, high levels of Foxp3 + Treg infiltration were more likely to be observed in pancreatic cancer tissues that had the Kras^{G12D} mutation, suggesting that Kras^{G12D} might contribute to the high level of Treg infiltration (Fig. 1E).

3.2. Mutant Kras converts CD4$^+$CD25$^-$ T cells into Tregs

Our study showed that Kras^{G12D} mutation in tumour tissues was associated with enhanced Treg infiltration. Whether Kras^{G12D} mutation was related to Treg infiltration, however, was unclear. To analyse the relationship of Kras^{G12D} and underlying mechanisms in pancreatic cancer, we isolated CD4$^+$ naïve T cells, then co-cultured them with Bxpc-3 and SW1990 cells, respectively. Results showed that Treg proportions were higher in SW1990 cells than in Bxpc-3 cells (Fig. 2A and B). SW1990 cells possess the Kras^{G12D} mutation, and Bxpc-3 cells express wild-type Kras (https://cancer.sanger.ac.uk/cosmic/). To further analyse the role of Kras^{G12D} mutation on Tregs, we employed Kras

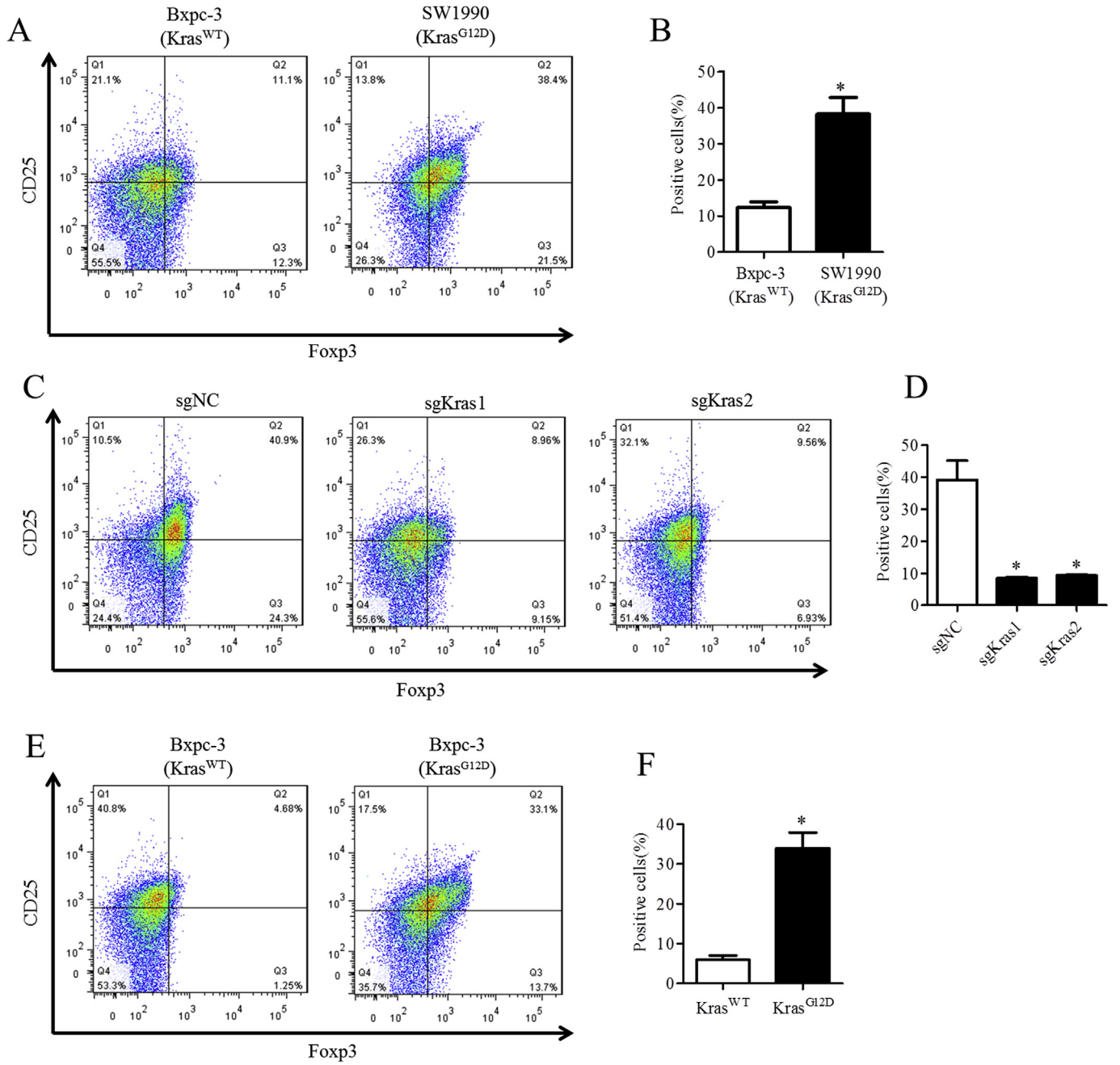

Fig. 2. Kras^{G12D} mutation promotes tumour-associated Treg conversion. (A) Flow cytometry analysis of tumour-associated Treg proportions after co-culturing of SW1990 cells with Kras^{G12D} mutation and Bxpc-3 cells with wild type Kras. (B) Statistical analysis of Treg proportions. (C) Flow cytometry analysis of tumour-associated Treg proportions after co-culturing of SW1990 cells with Kras knockout. (D) Statistical analysis of Treg proportions. (E) Flow cytometry analysis of tumour-associated Treg proportions after co-culturing of Bxpc-3 cells with Kras^{G12D} overexpression. (F) Statistical analysis of Treg proportions.

knockout SW1990 cells in co-culture with CD4$^+$ naïve T cells. Flow cytometry results showed that Treg proportions, as characterised by Foxp3 positive expression, was decreased in Kras knockout cells (Fig. 2C and D). In contrast, overexpression of Kras^{G12D} in Bxpc-3 cells increased Treg percentages (Fig. 2E and F). Therefore, from these results, we confirmed that Kras^{G12D} promotes the conversion of CD4$^+$ T cells to Tregs.

3.3. Kras^{G12D} mutation increases IL-10 and TGF-β levels

Treg infiltration in pancreatic cancer leads to tumour immune escape, leading to poor prognosis. IL-10 and TGF-β are secreted by many tumours and play important roles in Treg induction, therefore, we investigated whether Kras^{G12D} mutation regulated IL-10 and TGF-β levels. First, we analysed the mRNA levels of these genes in Bxpc-3 and SW1990 cells and found that IL-10 and TGF-β mRNA levels were higher in SW1990 cells than in Bxpc-3 cells (Fig. 3A and B). The IL-10 and TGF-β levels in cell supernatants were confirmed by ELISA. Consistent with the mRNA levels, IL-10 and TGF-β levels in SW1990 cell supernatants were higher than those in Bxpc-3 cells (Fig. 3C and D), further indicating that the levels of IL-10 and TGF-β are correlated with Treg conversion. Next, we investigated the expression and secretion levels of IL-10 and TGF-β in response to Kras^{G12D} knockout. Real-time PCR results showed that IL-10 and TGF-β mRNA levels were significantly decreased in sgKras1 and sgKras2 in SW1990 cells (Fig. 3E and F). Further, cell supernatants were collected for IL-10 and TGF-β cytokine

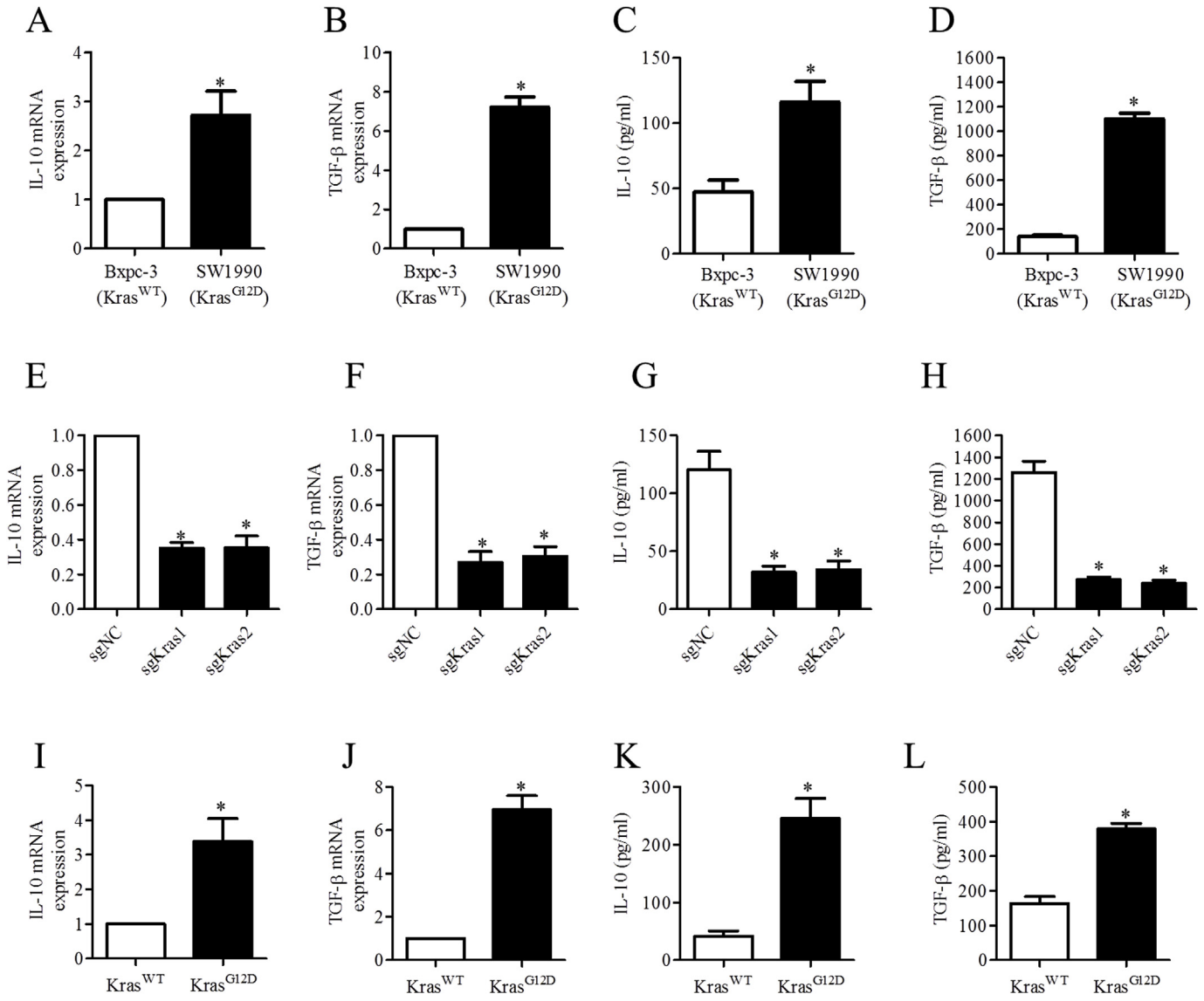

Fig. 3. Kras^{G12D} mutation up regulates IL-10 and TGF-β expression and secretion (A) and (B) Real-time PCR analysis of IL-10 and TGF-β expression in Bxpc-3 and SW1990 cells. (C) and (D) ELISA analysis of IL-10 and TGF-β levels in cell supernatants in SW1990 and Bxpc-3 cells. (E) and (F) Real-time PCR analysis of IL-10 and TGF-β mRNA levels in SW1990 cells with Kras knockout. (G) and (H) ELISA analysis of IL-10 and TGF-β levels in cell supernatants in SW1990 cells with Kras knockout. (I) and (J) Real-time PCR analysis of IL-10 and TGF-β mRNA expression in Bxpc-3 cells with Kras^{G12D} overexpression. (K) and (L) ELISA analysis of IL-10 and TGF-β levels in Bxpc-3 cell supernatants with Kras^{G12D} overexpression.

analysis, which showed that IL-10 and TGF-β levels were decreased after Kras^{G12D} knockout (Fig. 3G and H). This result indicates that Kras^{G12D} mutation plays a role in regulating IL-10 and TGF-β expression and secretion. In contrast, overexpression of Kras^{G12D} was also used to analyse IL-10 and TGF-β levels in Bxpc-3 cells. We found that overexpression of Kras^{G12D} mutation significantly increased IL-10 and TGF-β mRNA levels (Fig. 3I and J). Furthermore, the amount of IL-10 and TGF-β in cell supernatants also increased upon overexpression of the Kras^{G12D} mutant (Fig. 3K and L). Therefore, we considered that Kras^{G12D} mutation may up regulate IL-10 and TGF-β expression and secretion, thereby promoting Treg conversion.

3.4. IL-10 and TGF-β mediate Treg conversion induced by Kras^{G12D} mutation

The Kras^{G12D} mutation promoting conversion of CD4$^+$ naive T cells to Tregs was validated, but whether the conversion was primarily mediated by IL-10 or TGF-β in pancreatic cancer was uncertain. To address this question, we next analysed the roles of IL-10 and TGF-β in this process. We found that the proportion of Tregs was significantly increased after IL-10 treatment as well as after TGF-β treatment (Fig. 4A and B). However, when IL-10 or TGF-β was knocked down by siRNA in SW1990 cells and co-cultured with CD4$^+$ T cells, the proportion of Tregs decreased (Fig. 4C–F). These results confirmed that both IL-10 and TGF-β participate in the conversion of CD4$^+$ T to Tregs that is induced by Kras^{G12D} mutation.

3.5. The MEK/ERK pathway mediates the increase in IL-10 and TGF-β that is induced by Kras^{G12D} mutation

The mitogen-activated protein kinase/extracellular signal-regulated kinase (MEK/ERK) pathway is a key pathway that is downstream of Kras. We found that the MEK/ERK pathway was activated in response to Kras^{G12D} mutation. Specifically, Kras knockout decreased *p*-ERK1/2 levels (Fig. 5A). Then, we treated SW1990 cells with the MEK inhibitor PD98059 and found that the *p*-ERK1/2 level was significantly decreased

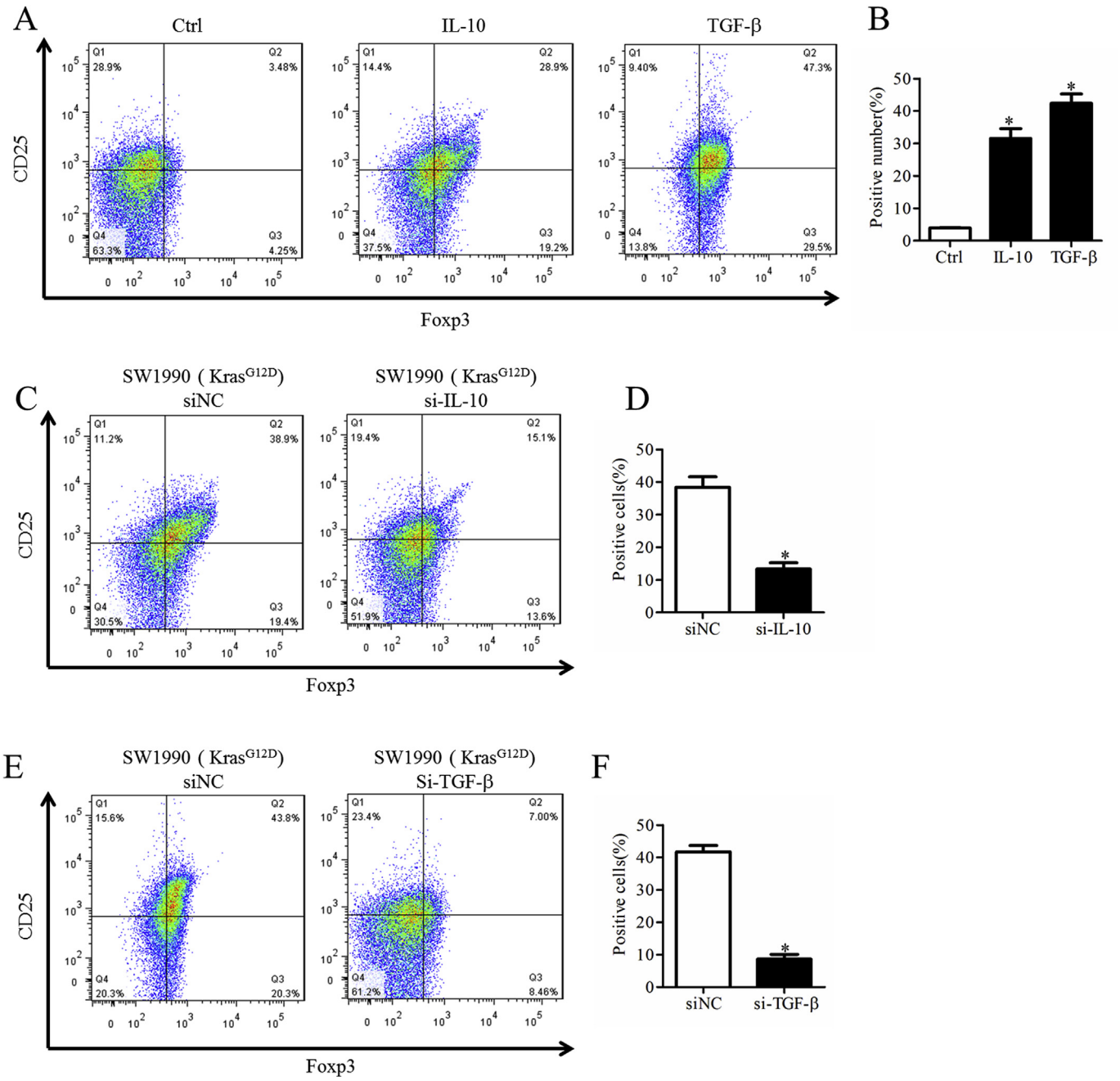

Fig. 4. IL-10 and TGF-β mediate the function of Kras^{G12D} mutation promoting Treg differentiation. (A) Flow cytometry analysis of tumour-associated Treg proportions after IL-10 and TGF-β treatment. (B) Statistical analysis of Treg proportions. (C) Flow cytometry analysis of tumour-associated Treg proportions after IL-10 knockdown by siRNA. (D) Statistical analysis of Treg proportions. (E) Flow cytometry analysis of tumour-associated Treg proportions after TGF-β knockdown by siRNA. (F) Statistical analysis of Treg proportions.

(Fig. 5B). Meanwhile, Real-time PCR showed that the IL-10 and TGF-β mRNA levels were also decreased (Fig. 5C and D), and this was confirmed by ELISA analysis, which showed decreased IL-10 and TGF-β expression (Fig. 5E and F). We next treated SW1990 cells with PD98059, followed by co-culture with CD4$^+$ naïve T cells and found that Treg proportions were decreased (Fig. 5G and H). Taken together, these findings indicated that Kras^{G12D} mutation activates the MEK/ERK pathway to increase IL-10 and TGF-β levels, which mediates the conversion of CD4$^+$ T cells to Tregs.

4. Discussion

Kras alteration is a classic landmark mutation that is involved in tumour initiation, maintenance, and progression. Mutated Kras in tumour cells promotes tumour growth, invasion, and metastasis by affecting cell cycle regulation, apoptosis, and other cellular processes [3]. In combination with other inactivating tumour suppressor gene mutations, the Kras mutation induces murine pancreatic cancer initiation and development in the classic mouse model of pancreatic cancer [14,15]. Kras^{G12D} and Kras^{G12V} are the most common mutations in the Kras gene in pancreatic cancer, and both are found in 30%–50% of pancreatic cancer tissues or ctDNA [16]. In this study, we found the Kras^{G12D} mutation in 35% of the resectable pancreatic cancer tissue samples, which is in line with other studies [16,17].

Tumour antigens include a wide variety of proteins that differ from those in normal cells. These proteins, such as mutated Ras, are closely

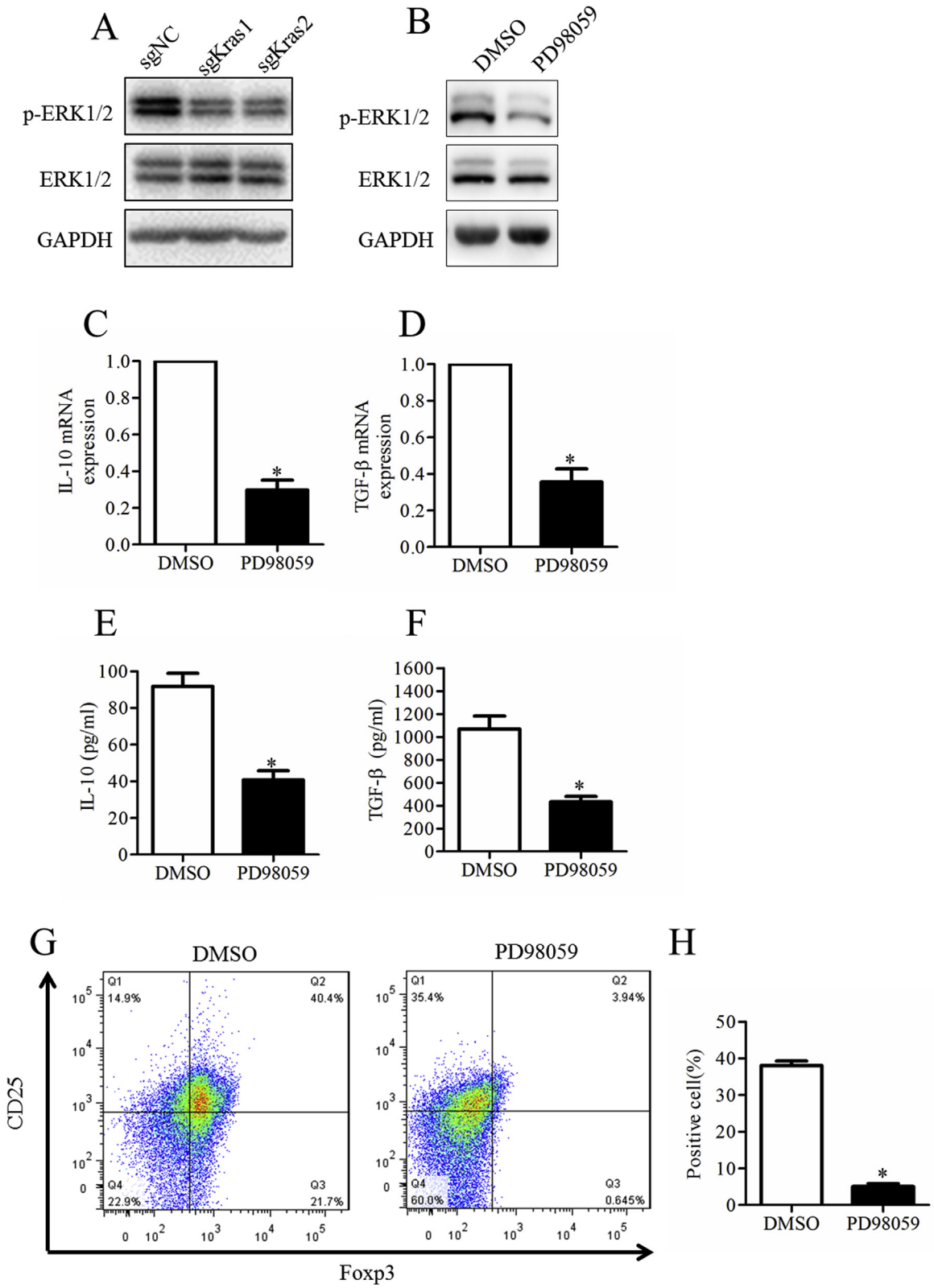

Fig. 5. The MEK/ERK signalling pathway participates in the progress of Kras^{G12D} mutation promoting Treg differentiation. (A) Western blot analysis of phospho-ERK1/2 levels in SW1990 cells with Kras knockout. (B) Western blot analysis of phospho-ERK1/2 levels in Bxpc-3 cells after PD98059 treatment. (C) and (D) Real-time PCR analysis of IL-10 and TGF-β expression in SW1990 cells after PD98059 treatment. (E) and (F) ELISA analysis of IL-10 and TGF-β level in SW1990 cell supernatant after PD98059 treatment. (G) Flow cytometry analysis of tumour-associated Treg proportions after PD98059 treatment. (H) Statistical analysis of Treg proportions.

linked to oncogenesis. As the most frequently mutated gene in pancreatic cancer, Kras has potential as an ideal target for immunotherapeutic treatments. The first Kras-related peptide-based vaccine showed that this immunotherapeutic approach is safe [18]. However, clinical trials showed that administration of synthetic Kras-derived peptides elicited a limited immune response in pancreatic cancer patients [19].

Due to the selection pressure of the immune microenvironment, tumour cells become less immunogenic over time. They often lose tumour and adaptive responses, resulting in immune evasion. Increasing evidence suggests that there is interplay between Kras mutations and immune disorder [20]. Notably, the $Kras^{G12V}$ mutation converts conventional T cells into Tregs *in vitro* in colon cancer, and knockout of Kras reduces the infiltration of Tregs in a Kras-driven lung tumourigenesis mouse model [11]. Further, mutated Kras is associated with suppressive Th1/cytotoxic T cell immunity in colorectal cancer [21], and lung cancer cells with the $Kras^{G12D}$ mutation induce $CD3^+$ T cells apoptosis [22]. In this study, we found that the $Kras^{G12D}$ mutation in tumour tissues was associated with high levels of Treg infiltration and that both Treg infiltration ($p = 0.002$) and $Kras^{G12D}$ mutation status ($p = 0.041$) in pancreatic cancer tissues was associated with overall survival (Supplementary Figure 1). Tumour cells that expressed mutated $Kras^{G12D}$ induced suppressive Tregs, and silencing of $Kras^{G12D}$ significantly reversed this effect. Meanwhile, transfection of $Kras^{G12D}$ into wild type tumour cells increased the proportion of Tregs.

Pancreatic cancer is considered one of the most evasive types of cancers, and pancreatic cancer cells downregulate the adaptive immune response against mutated antigens through a variety of mechanisms. Secretion of the immunosuppressive cytokines IL-10 and TGF-β by tumour cells is a critical factor for immune escape [23]. IL-10 inhibits T cell activation by suppressing IL-12 expression, which reduces T cell activation in and around the tumour in pancreatic cancer. TGF-β inhibits T cell activation and proliferation, inducing Treg differentiation in various cancers. Pancreatic cancer cells release TGF-β, directly reducing T cell activation and suppressing $CD8^+$ cytotoxic T lymphocyte (CTL)-mediated tumour killing [24]. Indeed, murine models of pancreatic cancer show increased survival when TGF-β is knocked out [25]. Tregs also suppress the T cell response by secreting the immunosuppressive cytokines TGF-β and IL-10 [26]. In this study, we found that pancreatic cancer cells with the $Kras^{G12D}$ mutation secreted higher levels of TGF-β and IL-10 than wild type pancreatic cancer cells. Moreover, knockout of the $Kras^{G12D}$ mutation in pancreatic cancer cells inhibited the secretion of TGF-β and IL-10, whereas overexpression of $Kras^{G12D}$ had the opposite effect.

Constitutive activation of the $Kras^{G12D}$ mutation stimulates various downstream effector pathways, such as the RAF/MEK/ERK and phosphatidylinositol 3-kinase/3-phosphoinositide-dependent protein kinase-1/AKT (PI3K/PDK1/AKT) pathways. This helps maintain tumour cell survival and allows tumour cell invasion and metastasis [3]. However, the mechanism underlying the effects of mutated Kras in regulating immune status in pancreatic cancer remains unclear. Interestingly, inhibition of MEK/ERK signalling enhances the expression of Foxp3 in a TGF-β dependent manner and induces Foxp3(+) Treg conversion [27]. Inhibition of MEK/ERK using pharmacological inhibitors reduces TGF-β production in breast tumour cells, supressing Treg augmentation in the tumour milieu [28]. In addition, a recent study demonstrated that the $Kras^{G12D}$ mutation increases the immunosuppressive marker PD-L1 by activating *p*-ERK signalling, thus attenuating T cell-mediated anti-tumour immunity [22]. Our data showed that the $Kras^{G12D}$ mutation promoted the production of IL-10 and TGF-β by activating the MEK/ERK pathway. Inhibition of MEK in pancreatic cancer cells with mutated Kras significantly decreased the secretion of IL-10 and TGF-β, thereby reducing the proportion of Tregs.

In summary, this study found that the $Kras^{G12D}$ mutation correlated with Treg infiltration in resectable pancreatic cancer tissues. We also found that the $Kras^{G12D}$ mutation mediated the upregulation of IL-10 and TGF-β secretion in tumour cells, notably, these are critical factors for Treg conversion. Furthermore, we demonstrated that Tregs increased in response to Kras overexpression via the MEK/ERK signalling pathway and that this could be reversed by MEK inhibitor treatment. Our study might provide a promising therapeutic option for pancreatic cancers with $Kras^{G12D}$ mutation.

Conflicts of interest

None.

Acknowledgements

This work was supported by the National Natural Science Foundation of China grants (81871940, 81802751) and The National Science Fund for Distinguished Young Scholars (81625016).

Appendix A. Supplementary data

Supplementary data to this article can be found online at https://doi.org/10.1016/j.canlet.2019.01.013.

References

[1] R.L. Siegel, K.D. Miller, A. Jemal, Cancer statistics, Ca - Cancer J. Clin. 2017 67 (1) (2017) 7–30.
[2] N. Waddell, M. Pajic, A.M. Patch, D.K. Chang, K.S. Kassahn, P. Bailey, et al., Whole genomes redefine the mutational landscape of pancreatic cancer, Nature 518 (7540) (2015) 495–501.
[3] S. Eser, A. Schnieke, G. Schneider, D. Saur, Oncogenic KRAS signalling in pancreatic cancer, Br. J. Canc. 111 (5) (2014) 817–822.
[4] A. Neesse, C.A. Bauer, D. Ohlund, M. Lauth, M. Buchholz, P. Michl, et al., Stromal biology and therapy in pancreatic cancer: ready for clinical translation? Gut (2018), https://doi.org/10.1136/gutjnl-2018-316451.
[5] C. Bauer, B. Kuhnemuth, P. Duewell, S. Ormanns, T. Gress, M. Schnurr, Prevailing over T cell exhaustion: new developments in the immunotherapy of pancreatic cancer, Cancer Lett. 381 (1) (2016) 259–268.
[6] A. Banerjee, A. Vasanthakumar, G. Grigoriadis, Modulating T regulatory cells in cancer: how close are we? Immunol. Cell Biol. 91 (5) (2013) 340–349.
[7] H. Cheng, G. Luo, Y. Lu, K. Jin, M. Guo, J. Xu, et al., The combination of systemic inflammation-based marker NLR and circulating regulatory T cells predicts the prognosis of resectable pancreatic cancer patients, Pancreatology : Official J. Int. Assoc. Pancreatol. 16 (6) (2016) 1080–1084.
[8] T. Hanke, N. Melling, R. Simon, G. Sauter, C. Bokemeyer, P. Lebok, et al., High intratumoral FOXP3(t) T regulatory cell (Tregs) density is an independent good prognosticator in nodal negative colorectal cancer, Int. J. Clin. Exp. Pathol. 8 (2015) 8227e35.
[9] Y. Tang, X. Xu, S. Guo, C. Zhang, Y. Tang, Y. Tian, et al., An increased abundance of tumor-infiltrating regulatory T cells is correlated with the progression and prognosis of pancreatic ductal adenocarcinoma, PLoS One 9 (2014) e91551.
[10] S.I. Abrams, S.N. Khleif, E.S. Bergmann-Leitner, J.A. Kantor, Y. Chung, J.M. Hamilton, et al., Generation of stable CD4+ and CD8+ T cell lines from patients immunized with ras oncogene-derived peptides reflecting codon 12 mutations, Cell. Immunol. 182 (2) (1997) 137–151.
[11] S. Zdanov, M. Mandapathil, R. Abu Eid, S. Adamson-Fadeyi, W. Wilson, J. Qian, et al., Mutant KRAS conversion of conventional T cells into regulatory T cells, Cancer Immunol. Res. 4 (4) (2016) 354–365.
[12] H. Cheng, C. Liu, J. Jiang, G. Luo, Y. Lu, K. Jin, et al., Analysis of ctDNA to predict prognosis and monitor treatment responses in metastatic pancreatic cancer patients, Int. J. Canc. 140 (10) (2017) 2344–2350.
[13] K. Fan, C. Yang, Z. Fan, Q. Huang, Y. Zhang, H. Cheng, et al., MUC16 C terminal-induced secretion of tumor-derived IL-6 contributes to tumor-associated Treg enrichment in pancreatic cancer, Cancer Lett. 418 (2018) 167–175.
[14] JPt Morris, S.C. Wang, M. Hebrok, KRAS, Hedgehog, Wnt and the twisted developmental biology of pancreatic ductal adenocarcinoma, Nat. Rev. Canc. 10 (10) (2010) 683–695.
[15] M.A. Collins, F. Bednar, Y. Zhang, J.C. Brisset, S. Galban, C.J. Galban, et al., Oncogenic Kras is required for both the initiation and maintenance of pancreatic cancer in mice, J. Clin. Invest. 122 (2) (2012) 639–653.
[16] H. Kinugasa, K. Nouso, K. Miyahara, Y. Morimoto, C. Dohi, K. Tsutsumi, et al., Detection of K-ras gene mutation by liquid biopsy in patients with pancreatic cancer, Cancer 121 (13) (2015) 2271–2280.
[17] T. Ogura, K. Yamao, K. Hara, N. Mizuno, S. Hijioka, H. Imaoka, et al., Prognostic value of K-ras mutation status and subtypes in endoscopic ultrasound-guided fine-needle aspiration specimens from patients with unresectable pancreatic cancer, J. Gastroenterol. 48 (5) (2013) 640–646.
[18] M.K. Gjertsen, A. Bakka, J. Breivik, I. Saeterdal, T. Gedde-Dahl 3rd, K.T. Stokke, et al., Ex vivo ras peptide vaccination in patients with advanced pancreatic cancer:

results of a phase I/II study, Int. J. Canc. 65 (4) (1996) 450–453.
[19] M.K. Gjertsen, A. Bakka, J. Breivik, I. Saeterdal, B.G. Solheim, O. Soreide, et al., Vaccination with mutant ras peptides and induction of T-cell responsiveness in pancreatic carcinoma patients carrying the corresponding RAS mutation, Lancet 346 (8987) (1995) 1399–1400.
[20] W.Q. Wang, L. Liu, H.X. Xu, C.T. Wu, J.F. Xiang, J. Xu, et al., Infiltrating immune cells and gene mutations in pancreatic ductal adenocarcinoma, Br. J. Surg. 103 (9) (2016) 1189–1199.
[21] N. Lal, B.S. White, G. Goussous, O. Pickles, M.J. Mason, A.D. Beggs, et al., KRAS mutation and consensus molecular subtypes 2 and 3 are independently associated with reduced immune infiltration and reactivity in colorectal cancer, Clin. Canc. Res. : Official J. Am. Assoc. Cancer Res. 24 (1) (2018) 224–233.
[22] N. Chen, W. Fang, Z. Lin, P. Peng, J. Wang, J. Zhan, et al., KRAS mutation-induced upregulation of PD-L1 mediates immune escape in human lung adenocarcinoma, Cancer Immunol. Immunother. CII 66 (9) (2017) 1175–1187.
[23] N. Martinez-Bosch, J. Vinaixa, P. Navarro, Immune evasion in pancreatic cancer: from mechanisms to therapy, Cancers 10 (1) (2018), https://doi.org/10.3390/cancers10010006.
[24] D.A. Thomas, J. Massague, TGF-beta directly targets cytotoxic T cell functions during tumor evasion of immune surveillance, Cancer Cell 8 (5) (2005) 369–380.
[25] J. Ellermeier, J. Wei, P. Duewell, S. Hoves, M.R. Stieg, T. Adunka, et al., Therapeutic efficacy of bifunctional siRNA combining TGF-beta1 silencing with RIG-I activation in pancreatic cancer, Cancer Res. 73 (6) (2013) 1709–1720.
[26] Y.D. Seo, V.G. Pillarisetty, T-cell programming in pancreatic adenocarcinoma: a review, Cancer Gene Ther. 24 (3) (2017) 106–113.
[27] L. Gabrysova, J.R. Christensen, X. Wu, A. Kissenpfennig, B. Malissen, A. O'Garra, Integrated T-cell receptor and costimulatory signals determine TGF-beta-dependent differentiation and maintenance of Foxp3+ regulatory T cells, Eur. J. Immunol. 41 (5) (2011) 1242–1248.
[28] D.M. Hossain, A.K. Panda, S. Chakrabarty, P. Bhattacharjee, K. Kajal, S. Mohanty, et al., MEK inhibition prevents tumour-shed transforming growth factor-beta-induced T-regulatory cell augmentation in tumour milieu, Immunology 144 (4) (2015) 561–573.